Supporting Information

Heteroarchitecturing a Novel Three-Dimensional Hierarchical MoO_2/MoS_2/Carbon Electrode Material for High-Energy and Long-Life Lithium Storage

Xufei Liu,[a,‡] Peng Mei,[b,‡,*] Yu Dou,[a] Rui Luo,[a] Yusuke Yamauchi[c,d,*] and Yingkui Yang[a,b,*]

[a] Key Laboratory of Catalysis and Energy Materials Chemistry of Ministry of Education & Hubei Key Laboratory of Catalysis and Materials Science, South-Central University for Nationalities, Wuhan 430074, China. E-mail: ykyang@mail.scuec.edu.cn

[b] Hubei Engineering Technology Research Centre of Energy Polymer Materials, School of Chemistry and Materials Science, South-Central University for Nationalities, Wuhan 430074, China. E-mail: meipeng@scuec.edu.cn

[c] Australian Institute for Bioengineering and Nanotechnology (AIBN) and School of Chemical Engineering, The University of Queensland, Brisbane, QLD 4072, Australia. E-mail: y.yamauchi@uq.edu.au

[d] JST-ERATO Yamauchi Materials Space-Tectonics Project and International Center for Materials Nanoarchitectonics (WPI-MANA), National Institute for Materials Science (NIMS), 1-1 Namiki, Tsukuba, Ibaraki 305-0044, Japan

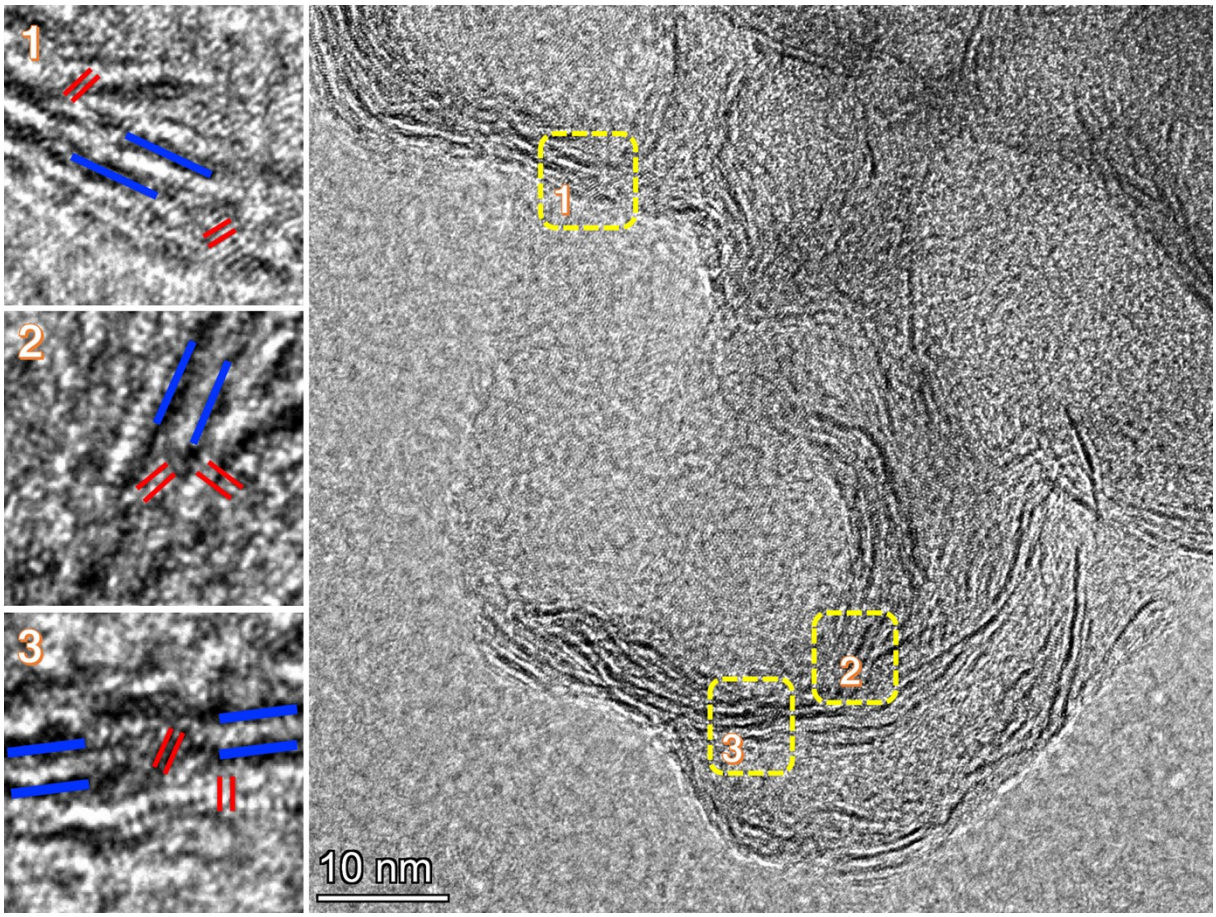

Figure S1 HRTEM image of $MoO_2/MoS_2/C$ with partial enlarged view of the lattice fringes, showing the coexistence of two crystalline phases. The red lines denote the lattice fringes of the MoO_2 phase, while the blue ones indicate the lattice fringes of the MoS_2 phase.

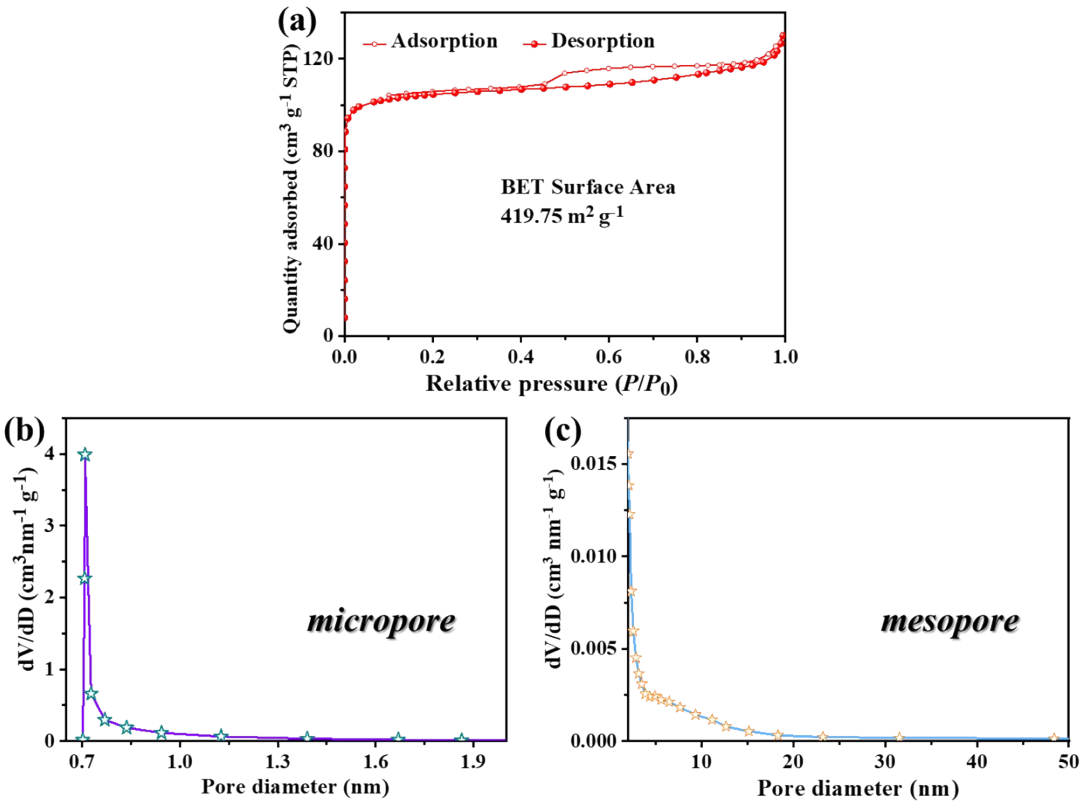

Figure S2 (a) N_2 adsorption–desorption isotherm, and (b, c) PSDs of $MoO_2/MoS_2/C$ in the micropore and mesopore ranges, respectively.

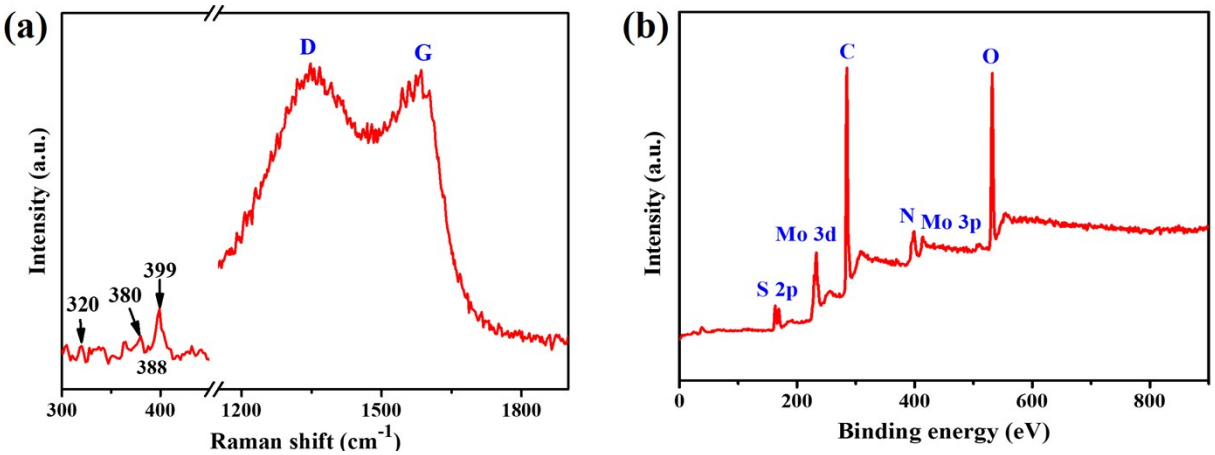

Figure S3 (a) Raman spectrum and (b) XPS spectrum of $MoO_2/MoS_2/C$.

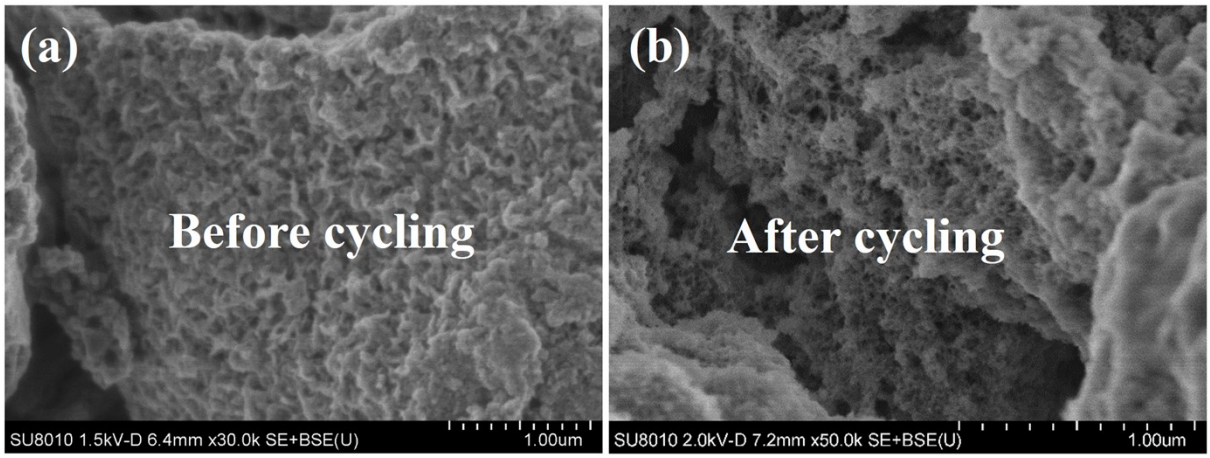

Figure S4 SEM images of the $MoO_2/MoS_2/C$ electrode before (a) and (b) after cycling at 5 A g^{-1} for over 2000 cycles.

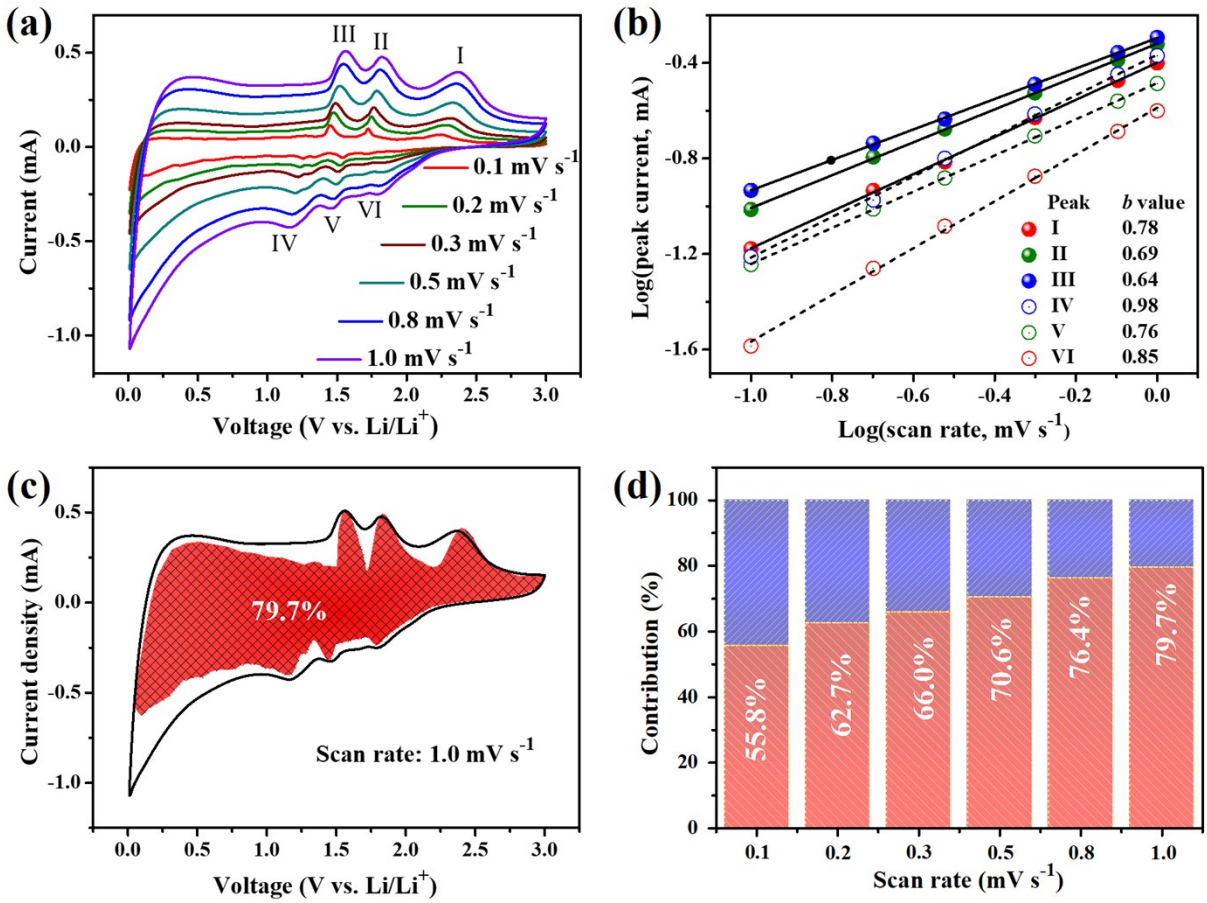

Figure S5 (a) CV curves at different scan rate. (b) Log *i* vs. log *v* plots at different oxidation and reduction states. (c) Separation of the capacitive and diffusion currents at a scan rate of 1.0 mV s^{-1}. (d) Normalized contribution ratio of capacitive and diffusion-controlled capacities at various scan rates.

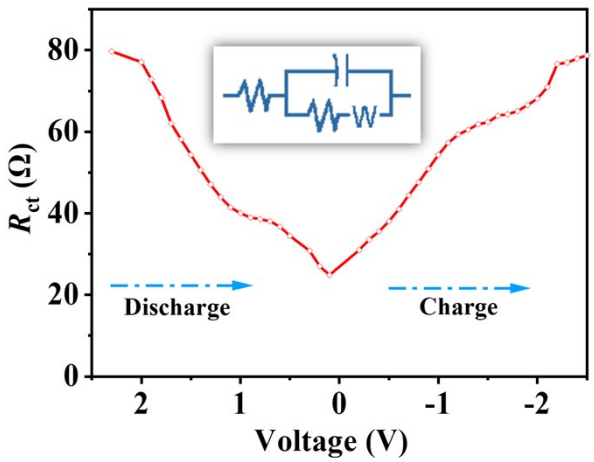

Figure S6 The fitting data of R_{ct} values at various charge/discharge voltages. The inset represents the equivalent circuit.

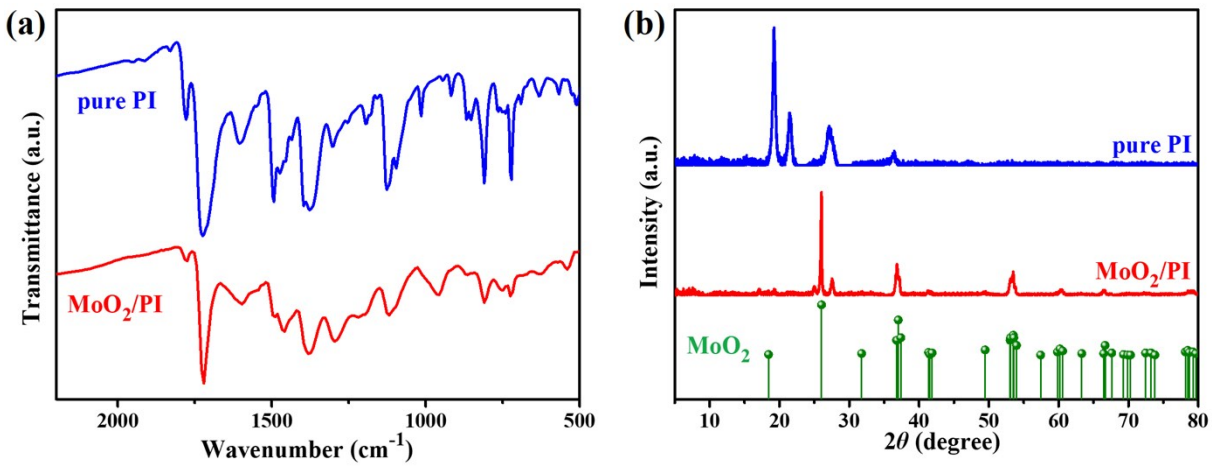

Figure S7 (a) FTIR spectra and (b) powder XRD patterns of the pure PI and MoO_2/PI precursors obtained after the hydrothermal polymerization.

Note for Figure S7: The appearance of the characteristic absorption peaks (the peaks of C=O at 1720 and 1778 cm^{-1}, and the peak of imide C-N at 1380 cm^{-1})[1] in the FT-IR spectra shown in Figure S7a clearly demonstrates the successful synthesis of PI in both cases. The XRD patterns in Figure S7b clarify the existence of both PI and MoO_2 crystal phases, indicating the successful synthesis of MoO_2/PI composite through the hydrothermal polymerization in the presence of PMo_{12}.[2]

Table S1 The elemental compositions of N-S-C obtained by XPS and CHNS analyses.

Sample	XPS analysis (atom%)				CHNS analysis (atom%)			
	C	**O**	**N**	**S**	**C**	**H**	**N**	**S**
N-S-C	**88.35**	**4.91**	**5.25**	**1.48**	**73.97**	**2.27**	**5.91**	**4.36**

References

1. X. Liu, S. Qiu, P. Mei, Q. Zhang and Y. Yang, *J. Mater. Sci.*, 2020, **56**, 3900-3910.
2. J. Xie, K. Zhu, J. Min, L. Yang, J. Luo, J. Liu, M. Lei, R. Zhang, L. Ren and Z. Wang, *Ionics*, 2019, **25**, 1487-1494.